学　位　論　文

Pigment epithelium-derived factor inhibits the growth of human esophageal squamous cell carcinoma by suppressing neovascularization.

（PEDF は血管新生を阻害することにより食道癌の増殖を抑制しうる）

北　海　道　大　学

角　谷　昌　俊

Title:

Pigment epithelium-derived factor inhibits the growth of human esophageal squamous cell carcinoma by suppressing neovascularization

Running title:

Anti-tumor effect of PEDF on human ESCC

Author:

Masatoshi Kadoya, Eiji Tamoto, Satoshi Hirano

Department of Gastroenterological Surgery II, Hokkaido University Graduate School of Medicine

Corresponding author:

Masatoshi Kadoya, Department of Gastroenterological Surgery II, Hokkaido University Graduate School of Medicine, North 15, West 7, Kita-ku, Sapporo, Hokkaido, 060-8638, Japan. Phone: 81-11-706-7714; Fax: 81-11-706-7158; E-mail: mkado.6809@kib.biglobe.ne.jp

Abstract

Introduction Neovascularization consists of angiogenesis and vasculogenesis during which bone marrow-derived endothelial progenitor cells (EPCs) are mobilized for blood vessel formation. Pigment epithelium-derived factor (PEDF) is known to be a potent inhibitor of angiogenesis in some solid carcinomas. However, the effects of PEDF on human esophageal squamous cell carcinoma (ESCC) and vasculogenesis are still unknown. The purpose of this research was to investigate the effect of PEDF on angiogenesis, tumor growth, and vasculogenesis in ESCC.

Materials and Methods The PEDF gene was transduced to the TE8 ESCC cell line not secreting endogenous PEDF and the HEC46 cell line originally secreting endogenous PEDF by lentivirus-based vectors expressing PEDF. *In vitro* endothelial cell proliferation and migration assays were performed using the supernatant derived from PEDF-overexpressing cells. In *in vivo* experiments, the effects of PEDF on chronological tumor growth, intratumoral microvessel density (MVD), tumor cell apoptosis, and the frequency of EPCs in peripheral blood and tumor tissues were examined in murine subcutaneous tumor models.

Results PEDF inhibited endothelial cell proliferation and migration *in vitro* and showed potent *in vivo* antitumor properties by inhibiting MVD in the human ESCC cell line that did not secrete endogenous PEDF. However, in the cell line secreting endogenous PEDF, additional PEDF gene transfer showed no inhibition of angiogenesis and no subsequent antitumor properties. With respect to vasculogenesis, PEDF was found to have potential to suppress vasculogenesis; the frequency of EPCs both in peripheral blood and tumor tissue was decreased in mice implanted with PEDF-overexpressing TE8 and HEC46 cells.

Conclusion PEDF may have potent antiangiogenic and antitumor effects in ESCC cells naturally not secreting endogenous PEDF and can be expected to be applied as gene therapy in the future.

Key words:
Pigment epithelium-derived factor
Esophageal squamous cell carcinoma
Angiogenesis
Vasculogenesis
Endothelial progenitor cell

Introduction

Although advances in surgical technique and perioperative management including multimodality therapy have improved the survival of esophageal squamous cell carcinoma (ESCC), it still remains a poor-prognosis carcinoma [1-3]. Therefore, novel adjuvant treatments are required for esophageal cancer patients in order to improve outcomes.

PEDF, a 50-kDa secreted glycoprotein and member of the serpin superfamily of serine protease inhibitors, was first purified from human retinal pigment epithelial cell-conditioned media as a factor with potent human retinoblastoma cell neuronal differentiating activity [4,5]. PEDF has recently been shown to be a potent inhibitor of both choroidal and retinal angiogenesis in animal models and has been identified as one of the most potent inhibitors of angiogenesis [6,7]. In regard to these anti-angiogenic and anti-tumor properties of PEDF, many reports have shown that PEDF has antitumor properties and antimetastatic activities based on its ability to inhibit angiogenesis [8-17].

It was previously indicated that low PEDF expression is associated with an increased risk of hepatic metastasis for patients with pancreatic adenocarcinoma and short survival on immunohistochemical analysis [18]. Furthermore, PEDF inhibits growth of tumor resulting from subcutaneously implanted human pancreatic adenocarcinoma cell lines in mice [19]. The antitumor effects of PEDF in ESCC remain unknown. However, it has been assumed that PEDF might show antiangiogenic effects regardless of the type of cancer. The antitumor effects of tumor angiogenesis inhibition are likely to be very effective in more hypervascular tumors, because neovascularization is essential for the growth and metastasis of solid tumors [6, 20].

Neovascularization consists of two distinct mechanisms of angiogenesis and vasculogenesis. Angiogenesis is defined as existing mature endothelial cells proliferating and migrating to form new blood vessels [21-24], and vasculogenesis is recognized as bone marrow-derived endothelial progenitor cells (EPCs) contributing to new blood vessel formation [21, 25-29, 30, 31]. It has been identified that PEDF effectively inhibits neovascularization, particularly angiogenesis. On the other hand, the effects of PEDF on EPCs and EPC-mediated vasculogenesis have not been sufficiently demonstrated, but there was a report that a PEDF-derived peptide blocks mobilization of bone marrow-derived EPCs during retinal neovascularization [32]. Furthermore, the effects of PEDF on EPCs in tumor tissues were also reported [33-36], but its situation remains uncertain. Therefore, in the current experiment, the antiangiogenic property of PEDF transferred to human ESCC cell lines and the effect of PEDF on EPCs in the peripheral blood and tumor tissues were investigated. To the best of our knowledge, this is the first report to clarify the antitumor effects of PEDF on ESCC and the effects of PEDF on EPCs.

Materials and methods

Cell lines and mice.

Human non-cancer cell line Het1A was purchased from American Type Culture Collection (Manassas, VA). Human esophageal squamous cell cancer (ESCC) cell lines TE2, TE5, TE8, TE10, and TE13 were generously provided by Dr. Nishihira (University of Tohoku, Japan). Human ESCC cell line HEC46 was provided by Dr. Toge (University of Hiroshima, Japan), and SGF7 was provided by Toyama Medical and Pharmaceutical University. The cell lines were propagated in monolayer cultures in Dulbecco's modified Eagle's medium (DMEM) for the TE series and RPMI 1640 medium for HEC46 and SGF7, supplemented with 10% fetal bovine serum, 1% penicillin/streptomycin. Human Umbilical Vein Endothelial Cells (HUVECs) and Human Microvascular Endothelial Cells (HMVECs) were purchased

from Kurabo (Osaka, Japan) and maintained in HuMedia-EG2 medium and HuMedia-MvG medium, respectively, according to the manufacturer's instructions. These cell lines were incubated at 37°C in humidified air containing 5% CO_2.

Four to six-week-old female BALB/c-nu/nu mice and C.B-17 SCID mice were purchased from Japan Charles River Laboratory (Tokyo, Japan) and maintained under specific pathogen-free conditions. All animal procedures were conducted according to guidelines provided by the Hokkaido University Institutional Animal Care and Use Committee under an approved protocol.

Preparation of Supernatant Derived from Cancer Cell Lines.

A total of 2×10^6 cells were seeded on 100-mm cell culture dishes. Then, cells were rinsed briefly two times with PBS and rinsed with serum-free medium for 4 hours. Cells were then incubated in fresh serum-free 10-mL medium for 48 hours, and the supernatant and lysate were collected separately. The supernatants were centrifuged to remove cell debris and concentrated and dialyzed using 0.45 μm PVDF membrane filters (Millipore Corporation, Bedford, MA).

Western blot analysis.

Samples were resolved using 15% SDS-PAGE and then transferred to a nitrocellulose membrane (Amersham, Aylesbury, United Kingdom) for Western blot analysis. A monoclonal mouse anti-human PEDF antibody (Trans Genic, Kumamoto, Japan) was used as the primary antibody, and a goat anti-mouse immunoglobulin G (Jackson ImmunoResearch Laboratories, West Grove, PA) was used as the secondary antibody. Immunoreactivity was detected by an enhanced chemiluminescence detection system (Amersham). Recombinant human PEDF peptide, with molecular weight of 50 kDa, was used as the positive control (Upstate, Lake Placid, NY).

Construction of PEDF expression lentiviral vector.

The human PEDF cDNA was originally cloned from a human splenic cDNA library (Clontech, Palo Alto, CA) and inserted into an entry vector, pENTR2B (Invitrogen). PEDF and GFP expression lentiviral vector (LV-PEDF) and PEDF lacking and GFP expression control vector (LV-GFP) were constructed using the ViraPower Lentiviral System (Invitrogen), as described previously [19].

Lentiviral transduction of human ESCC cell lines

TE8 and HEC46 cells were plated in 60-mm cell culture dishes at a density of approximately 70% confluence and allowed to attach overnight for lentiviral transduction. Three times every 12 hours, the medium was replaced with 1 mL fresh complete medium, 300 μL lentiviral supernatant, and 8 μg/mL hexadimethrine bromide (Sigma, St. Louis, MO) to assist in the uptake of viral particles. Then, 48 hours after the third transduction, the cells were cultured in full growth medium containing blasticidin (Invitrogen) for selection of transductants. LV-PEDF-transduced human ESCC cell lines (TE8P and HEC46P) and LV-GFP-transduced cell lines (TE8G and HEC46G) were collected at 10 days after blasticidin selection.

In vitro proliferation assay.

A proliferation assay was planned to assess the effect of PEDF on cell proliferation. A total of 5×10^3 HUVECs or

HMVECs were resuspended in 100 μL culture medium, seeded in each well of a 96-well culture dish and preincubated. Then, 100 μL of supernatant derived from TE8-wild-type (TE8WT), TE8-infected LV-GFP (TE8G), TE8-infected LV-PEDF (TE8P) and HEC46WT, HEC46G, and HEC46P cells, and 100 μL of HuMedia-EG2 medium or HuMedia-MvG medium were added, respectively. Then, 72 hours later, the proliferation rate was assessed using the Cell Counting Kit 8 (Wako Chemicals, Osaka, Japan). The absorbance value of each well was determined at 450 and 600 nm using a microplate reader (Molecular Devices, Tokyo, Japan).

In vitro migration assay.

The effect of the supernatant from TE8P and HEC46P cell lines on the migration of endothelial cells was examined using a modified double-chamber migration assay. Inserts (8-μm pores; Costar) coated with rat tail collagen type Ⅰ for 24-well culture dishes were used as the upper chamber. HUVECs or HMVECs at passages 4 to 6 were resuspended in HuMedia-EG2 medium or HuMedia-MvG medium, respectively, and 1×10^4 cells in 250 μL medium were seeded into the upper chamber and preincubated. The lower chamber was filled with 600 μL of supernatant from TE8WT, TE8G, TE8P and HEC46WT, HEC46G, and HEC46P cells. These chambers were incubated at 37°C in humidified air containing 5% CO_2 for 5 hours to allow the cells to migrate through the collagen-coated membranes. After the non-migrated cells were scraped from the upper surface of the membrane, the membrane was stained with Diff-Quick Solution (Sysmex, Kobe, Japan). The number of stained cells was determined by microscopic counting of the cells in six random fields in each well under a microscope at ×200 magnification.

In vivo growth of PEDF-overexpressing cells in a subcutaneous cancer cell-implant model.

TE8 cells (4×10^6 cells, WT, G, P) and HEC46 cells (2×10^6 cells, WT, G, P) were implanted subcutaneously into the left flanks of BALB/c-nu/nu mice. The tumors were monitored every day and their sizes measured every 7 days after implantation. The tumor volume was calculated as follows: tumor volume = length×width^2×0.5. The animals were sacrificed 28 days after subcutaneous injection, and the tumors were analyzed.

Immunohistochemistry.

Immunohistochemical reactions were carried out by the streptavidin-biotin-peroxidase method to verify overexpression of PEDF and GFP in tumor tissues of each group. Each slide was deparaffinized with xylene, rehydrated through a graded series of ethanol/water, and treated with pH8 EDTA buffer in a pressure cooker for 2 minutes. The slides were immunostained using the Ventana ES automated immunohistochemistry system (Ventana Medical Systems Japan, Yokohama, Japan). The protocol was based on an indirect biotin-avidin system and used a universal biotinylated immunoglobulin secondary antibody, diaminobenzidine substrate, and hematoxylin counterstain. Unstained sections were incubated for 32 minutes at 37°C with a mouse anti-human PEDF monoclonal antibody (Chemicon International, Temula, CA; 1:200 dilution) or monoclonal rabbit anti-GFP antibody (Chemicon International; 1:500 dilution). These antibodies were detected by adding biotinylated goat anti-mouse antibody, avidin-biotin complex, and 3,3'-diaminobenzidine (Ventana DAB Universal Kit, Ventana-Bio Tek Solutions, Tucson, AZ). The sections were then counterstained in hematoxylin for 1 minute and mounted in Permount (Microslides, Muto-Glass, Tokyo, Japan). As a positive control, retinal pigment epithelial cells, which are known to react strongly to PEDF, were used. As negative controls, 10% normal mouse serum was used as the primary antibody.

Microvessel staining and counting.

To evaluate the anti-angiogenic activity of PEDF, quantification of intratumoral microvessel density was performed by immunohistochemical analysis. The staining process was similar to that used for PEDF. Intratumoral microvessels were detected using a monoclonal rat anti-mouse CD34 antibody (HyCult Biotechnology, Uden, The Netherlands). The antibody was used at a 1:10 dilution in antibody diluent (Dako-Cytomation, Carpinteria, CA). The areas of highest microvessel density were chosen using low-power light microscopy. These areas, referred to as hotspots, were found by scanning the tumor sections at a total magnification of ×40. Once the hotspot was selected, microvessel counts were then performed by two independent observers at this area of highest neovascularization. The microvessel counts were determined at a total magnification of ×200. In all samples, the mean value of the number of microvessels was calculated from five independent fields.

Quantitative analyses of apoptosis in PEDF-overexpressing cells in a subcutaneous tumor model.

The antitumor efficacy of PEDF was investigated by quantitative analyses of apoptosis. Four-μm-thick sections from paraffin-embedded tumor sections were assayed by the terminal deoxynucleotidyl transferase–mediated dUTP nick end labeling (TUNEL) method using an apoptosis in situ detection kit (Wako Chemicals, Osaka, Japan) according to the manufacturer's protocol. Briefly, deparaffinized sections were washed with distilled water and treated with Protein Digestion Enzyme for 5 min at 37°C. After washing with four changes of PBS, sections were treated with TdT solution, incubated with 3% hydrogen peroxide for 5 min to block endogenous peroxidase activity, and then treated with peroxidase-conjugated antibody for 10 min at room temperature. After washing in PBS, nick end labeling was visualized by immersing reacted sections in 3,3'-diaminobenzidine solution and counterstaining with methyl green. As a negative control, the tissue sections were incubated with TdT buffer that did not contain the enzyme. For the positive control, tissue sections were treated with DNase Ⅰ prior to treatment with TdT. In each sample, the ratio of the TUNEL-positive area to the total area (Apoptotic Area Ratio; AAR) was measured using NIH image (ver.1.61) at low magnification. Then, viable tumor volume (VTV) was approximately calculated as the tumor volume at 28 days × (100-AAR) × 1/100.

Flow cytometric analysis of peripheral blood mononuclear cells (PBMCs) and endothelial progenitor cells (EPCs) in peripheral blood of a subcutaneous cancer cell-implant model.

Fluorescence activated cell sorting (FACS) analysis was performed to compare the frequency of endothelial progenitor cells (EPCs) in each subcutaneously implanted model. Mice were bled from the right axillary vein, and peripheral blood mononuclear cells (PBMCs) were obtained from the whole blood of the mouse at 28 days by density centrifugation using Histopaque-1077 (Sigma-Aldrich, St. Louis, MO). After the red blood cells were lysed with an ammonium chloride lysing buffer, PBMCs per mL in peripheral blood were counted for the calculation of EPCs per mL in peripheral blood afterward. Then, PBMCs were incubated for 30 minutes at 4°C with fluorescein isothiocyanate (FITC) conjugated rat anti-mouse Prominin Ⅰ antibody (eBioscience Inc., San Diego, CA), R-phycoerythrin (R-PE) conjugated rat anti-mouse Flk-1 antibody (BD PharMingen, San Diego, CA), and allophycocyanin (APC) conjugated rat anti-mouse CD45 antibody (BD PharMingen). Isotype-matched rat immunoglobulin (BD PharMingen) served as a negative control. After centrifugation and washing, the cells were transferred to FACS tubes and fixed in 2% paraformaldehyde for FACS analysis on a FACSCalibur flow cytometer and CellQuest software (Becton Dickinson Immunocytometry Systems, San

Jose, CA). PBMC and EPC evaluations were performed by enumeration using four-color flow cytometry. First, cell suspensions were evaluated by a FACSCalibur using analysis gates designed to exclude debris, dead cells, and platelets (Fig. 1A). After acquisition of at least 100,000 cells per sample, CD45+ cells (hematopoietic cells) were excluded by using appropriate analysis gates (Fig. 1B). Secondly, prominin I+, Flk-1+, CD45- cells (EPCs) were evaluated using appropriate analysis gates. Percentages of prominin I and Flk-1 dual-staining cells were compared with appropriate negative controls (Fig. 1C). The upper right quadrant population identifies prominin I+, Flk-1+, CD45- cells (EPCs), which can be measured as a percentage of EPCs (Fig. 1D). The number of EPCs per mL in peripheral blood was calculated from a percentage of EPCs and the number of PBMCs per mL in peripheral blood.

Immunofluorescence staining of EPCs in subcutaneous tumor tissues.

To examine the frequency of EPCs in tumor tissues of each group, frozen sections were prepared for fluorescence microscopic examinations. The mice were implanted with each cell line subcutaneously and sacrificed at 28 days, and tumor tissues were isolated and embedded in Tissue-Tek OCT 4583 compound (Sakura, Tokyo, Japan), and snap-frozen in liquid nitrogen to examine them for the presence of EPCs in the tumor tissues. Then, 4-μm-thick sections were fixed with cold acetone, and the samples were washed three times with PBS and incubated for 30 min at room temperature with a protein blocking solution consisting of PBS containing 2% normal goat serum and 5% normal sheep serum. Excess blocking solution was drained, and the samples were incubated for 24 h at 4°C with a 1:100 dilution of FITC conjugated rat anti-mouse CD31 antibody (BD PharMingen). The samples were then rinsed four times with PBS and incubated for 24 h at 4°C with a 1:100 dilution of phycoerythrin (PE) conjugated rat anti-mouse prominin I (eBioscience Inc., San Diego, CA). The slides were rinsed with PBS and counterstained for 5 min at room temperature with 4', 6-diamidine-2'-phenylindole dihydrochloride (DAPI; Roche Diagnostics, Indianapolis, IN). The sections were then rinsed with distilled water and mounted in Vectashield mounting medium (Vector Laboratories, Inc, CA), and stored at 4°C until use. As negative controls, isotype-matched rat immunoglobulin (BD PharMingen) was used. In each subcutaneous model, the expression of endothelial cell antigen CD31 and bone marrow-derived cell antigen prominin I were clarified by immunofluorescence staining. On the merged image of CD31 and prominin I, tumor blood vessels containing EPCs stained yellow. The frequency of EPCs in tumor vessels was quantified by the ratio of fields contained EPCs to total 25 fields per tissue sample at least two slides per each group at ×200 magnification. The EPC frequency was determined by two independent observers. Images of immunofluorescently labeled sections were obtained with a fluorescence microscope (Olympus AX80) equipped with a cooled CCD camera (Olympus DP71, Tokyo, Japan). All images were analyzed with Adobe Photoshop 6.0 software (Adobe Systems, San Jose, CA).

Statistical analysis.

All values are presented as medians ± range. Significance was evaluated using the Mann-Whitney *U* test, and in subcutaneous tumor models, analysis of covariance was also used; $P < 0.05$ was considered significant.

Results

PEDF expression in human esophageal squamous cell carcinoma and non-carcinoma cell lines.

The endogenous PEDF protein expression levels in the human esophageal non-cancer cell line Het1A and seven kinds

of human ESCC cell lines were screened beforehand by Western blotting analysis (data not shown). On the basis of this result, two cancer cell lines were selected for this investigation. One was TE8, which does not endogenously secrete PEDF protein, and the other was HEC46, which endogenously secretes PEDF protein (Fig. 2).

PEDF expression in human esophageal squamous cell carcinoma after lentivirus-mediated gene transfer.

The lentiviral construct that included human PEDF cDNA used in this experiment was previously described (20). To examine whether PEDF gene was successfully transferred to TE8 and HEC46 cells by lentivirus and secreted in lentivirus-infected cells, Western blotting was used. The supernatant and lysate from TE8 and HEC46 cell lines that were infected with either LV-PEDF or the control vector LV-GFP were analyzed. Lentivirus-mediated gene transfer that used LV-PEDF and the control vector LV-GFP was achieved successfully, and PEDF protein was strongly observed in both TE8P and HEC46P (Fig. 2). As the band of the sample from the supernatant was recognized to be denser than that from the lysate, the supernatant was used in the following experiments.

Anti-proliferative and migration inhibitory effect of PEDF on endothelial cells.

The supernatant from TE8WT and TE8G cells significantly promoted the proliferation of HUVECs and HMVECs, and the supernatant from TE8P cells significantly inhibited the proliferation of both HUVECs and HMVECs as compared with the supernatant from TE8WT or TE8G cells (Fig. 3A). On the other hand, the supernatant from HEC46WT and HEC46G cells did not promote the proliferation of HUVECs and HMVECs. Although the supernatant from HEC46P cells significantly suppressed the proliferation of HUVECs as compared with the supernatant from HEC46WT or HEC46G cells, the supernatant from HEC46P cells did not suppress the proliferation of HMVECs as compared with the supernatant from HEC46WT or HEC46G cells (Fig. 3B). The migrations of both HUVECs and HMVECs were significantly stimulated by the supernatant from TE8WT and TE8G cells and inhibited by the supernatant from TE8P cells in comparison with the supernatant from TE8WT or TE8G cells (Fig. 3C). In the HEC46 series, the supernatant from HEC46WT, HEC46G, and HEC46P did not stimulate the migrations of HUVECs and HMVECs (Fig. 3D).

In vivo growth of PEDF-overexpressing cells in subcutaneous tumor models.

The impact of PEDF overexpression on tumor growth in TE8 cells and HEC46 cells *in vivo* was examined using subcutaneous tumor models. As shown in Fig. 4A and B, tumors grew rapidly in the models implanted with untransduced and GFP-transduced TE8 cells, but tumor grew significantly more slowly in the model implanted with PEDF-overexpressing TE8 cells. Overexpression of PEDF was demonstrated in xenograft tumor tissue by immunohistochemistry (Fig. 4C). The intratumoral microvessel density in tumor tissues derived from subcutaneously TE8P cell-implanted mice showed a marked reduction compared with TE8WT or TE8G cell-implanted mice (Fig. 4D, E). As shown in Fig. 4F, there was no difference in tumor growth among HEC46WT, HEC46G, and HEC46P cells despite PEDF overexpression in HEC46P cells (Fig. 4G). The intratumoral microvessel density did not differ among HEC46WT, HEC46G, and HEC46P cells (Fig. 4H, I). PEDF gene transferred to HEC46 cells had no effect on angiogenesis. The microvessel density of tumor tissues from TE8WT cells was significantly more abundant than that of HEC46WT cells (Fig. 4J).

Evaluation of apoptotic change in subcutaneous cell implant models.

The apoptotic area ratio (AAR) of tumor sections from PEDF-overexpressing TE8 cells was significantly greater than that of TE8WT and TE8G cells. In relation to this result, viable tumor volume (VTV) in tumor implanted with PEDF-overexpressing cells was significantly lower than in tumor implanted with TE8WT and TE8G cells. On the other hand, there was no difference in AAR or VTV among the tumors implanted with HEC46WT, HEC46G, and HEC46P cells (data not shown).

Measurement of EPCs in Peripheral Blood by Flow Cytometry and Contributions of EPCs to Tumor Vessel Formation.

The amount of PBMCs from TE8WT and HEC46WT-bearing mice was more abundant than that from non-tumor-bearing mice (Fig. 5A, B). The amount of PBMCs from TE8P-bearing mice was significantly smaller than that from TE8WT or TE8G bearing mice (Fig. 5A). On the other hand, there was no difference in the amount of PBMCs among HEC46WT, HEC46G and HEC46P bearing mice (Fig. 5B). The amount of EPCs in peripheral blood from TE8WT-bearing mice was more abundant than that from non-tumor-bearing mice, and the amount of EPCs in peripheral blood from TE8P-bearing mice was significantly smaller than that from TE8WT or TE8G-bearing mice (Fig. 5A). The amount of EPCs in peripheral blood from HEC46P-bearing mice was also significantly lower than that from HEC46WT or HEC46G-bearing mice (Fig. 5B). The incorporation of EPCs into each tumor tissue is shown in the representative fluorescence microscopic photographs (Fig 5C, D). In connection with the reduction of EPCs in peripheral blood from PEDF-overexpressing cell-bearing mice, the recruitment of EPCs into tumor tissue was significantly decreased in tumor tissue from PEDF-overexpressing TE8 and HEC46 cells-bearing mice than in that from WT and G cell-bearing mice (Fig. 5E).

Discussion

Conquering ESCC remains a major clinical problem to be solved. Existing multimodality treatments including surgical resection, adjuvant chemotherapy, and radiotherapy have provided unsatisfactory responses for several decades [1-3]. Thus, development of novel therapeutic strategies for ESCC is required.

Angiogenesis has been already recognized to play an important role in accelerating tumor growth [20-24]. Recently, it has been reported that increasing PEDF expression levels in tumor tissue resulted in suppression of tumor growth and metastasis in various epithelial cancers in some animal models. This was mainly caused by the antiangiogenic effect of PEDF. Inhibition of intratumoral angiogenesis as a result of suppression of endothelial cell proliferation and migration by PEDF led to facilitation of cancer cell apoptosis [9-17, 19, 37]. In the present study, it was demonstrated for the first time that PEDF also has antiangiogenic and antitumor effects against ESCC cells.

Neovascularization consists of two mechanisms, angiogenesis and vasculogenesis. Vasculogenesis controlled by keeping a balance between pro- and anti-angiogenic factors is an important mechanism of neovascularization [38, 39]. From the results of measurements of EPCs by flow cytometry, EPCs in peripheral blood were significantly induced in TE8WT-implanted mice, and they were suppressed by PEDF gene transfer. In HEC46 cells, although a significant increase of EPCs was not found in HEC46WT-implanted mice, the number of EPCs was significantly decreased by PEDF. From the result of immunofluorescence staining, the incorporation of EPCs into tumor vessel formation was also suppressed by PEDF gene transfer in both TE8 and HEC46 cell-implanted tumor tissues. These data suggest that PEDF

has potential to inhibit vasculogenesis, but it was thought that PEDF might have two mechanisms of inhibition of vasculogenesis: it might suppress the release of whole PBMCs including EPCs from bone marrow to peripheral blood in TE8, and it might directly inhibit the release of only EPCs from bone marrow to peripheral blood without affecting the number of PBMCs in HEC46. Supporting this, although no data were obtained in this experiment, some further verification, for example, the acceleration of EPC proliferation in bone marrow of WT cell-implanted mice, EPC mobilization from bone marrow to circulation, the incorporation of EPCs to intratumoral vessels, the differentiation of incorporated EPCs to mature endothelial cells, and the successive estimation of direct inhibitory effects of PEDF on these accelerations are desired.

However, in HEC46 cells, the investigation for sections of intratumoral EPCs was inconsistent with the aforementioned in vivo effects of PEDF on intratumoral vessels and tumor growth. The reason that there was no difference in tumor growth among HEC46WT, G, and P, despite successful inhibition of vasculogenesis, might be due to the possibility that tumor growth would originally not depend on vasculogenesis as much, because a significant increase of EPCs in peripheral blood was not observed in HEC46WT-implanted mice compared to control mice, unlike with TE8WT cells. Furthermore, this discrepancy may have its origin in the possibility that, since the proportion of angiogenesis is greater in neovascularization, even if a small proportion of vasculogenesis is inhibited by PEDF, the anti-tumor effect will not be evident. However, further examinations are needed to confirm this.

In the *in vivo* experiment, although the number of PBMCs increased in both WT tumor-bearing mice, it is thought that antitumor immunity may participate in the increase of PBMCs in tumor-bearing mice. That is, it is thought that it is possible for the increase of PBMCs to be brought about by the activation of the immune mechanism for tumor cells in the tumor-bearing state, and that it is possible for the declining number of PBMCs in PEDF-overexpressing tumor bearing-mice not only to be related to the efficacy of PEDF, but also to correlate with the absolute amount of tumor.

PEDF seems to possess both antiangiogenic and antivasculogenic effects and suppresses tumor growth by inhibiting neovascularization. However, in ESCC cell lines secreting endogenous PEDF, intratumoral angiogenesis is thought to be already in an inhibitory state of neovascularization with its lower intratumoral microvessel density. There is also the possibility that even if exogenous PEDF is introduced into such cell lines, the additional antiangiogenic effect of PEDF will not be shown, and the mechanism for inducing tumor tissues to apoptosis is also disturbed. These data suggest that ESCC cell lines secreting endogenous PEDF may acquire some faculty that enables tumors to grow without neovascularization.

Recently, some reports have indicated that PEDF not only inhibits angiogenesis, but it also has the ability to induce apoptosis in tumors [40, 41]. The mechanism of PEDF-induced apoptosis in malignant tumors has not yet been sufficiently elaborated. However, it is thought that a functional epitope on the PEDF protein, which increases cell death in prostate carcinoma *in vitro* with the 34-mer peptide, would have the capacity to show apoptotic activity [42]. However, as in the present experiments, treatments that used full-length PEDF *in vitro* have shown significant tumor cell apoptosis in some malignant cells [11, 19, 41]. According to quantitative analyses of apoptosis with the measurement of AAR and VTV in tumor tissue, PEDF induced apoptosis in carcinoma cells and decreased viable carcinoma cells. With respect to PEDF-induced apoptosis, mechanisms promoting endothelial cell apoptosis in newly remodeling tumor vessels rather than existing mature vessels and inducing immediate tumor epithelial cell apoptosis have been described [37]. PEDF may be thought to have an antitumor effect by not only inhibiting neovascularization but also by directly inducing tumor cell apoptosis in human ESCC. However, in tumor cells secreting endogenous PEDF, the apoptotic effect induced by

PEDF gene transfer was weak, and viable carcinoma cells completely remained in tumor tissue. These results may suggest that factors other than angiogenesis and vasculogenesis have stronger effects on multiplication of tumor cells in the case of ESCC cells that endogenously secrete PEDF.

In conclusion, PEDF has potential for potent antiangiogenic and antitumor properties against human ESCC, especially that lacking endogenous PEDF. In the future, PEDF is expected to be used as novel gene therapy for the treatment of ESCC. However, investigation of PEDF expression in ESCC tumor tissue is needed to select patients who would benefit from suitable PEDF gene therapy as tailor made therapy.

Acknowledgment

The authors would like to thank the late Dr. Satoshi Kondo and the late Dr. Masaki Miyamoto (Department of Gastroenterological Surgery II, Division of Surgery, Hokkaido University Graduate School of Medicine) for their great contribution to this research. The authors would also like to thank Hiraku Shida, Rika Osanai, and Naomi Saitoh for their technical support in immunohistochemical analyses, and Dr. Jiro Arikawa and Tsutomu Osanai for their advice on animal experiments. Without their support, submission of this manuscript would not have been possible.

References

1. Lerut T, Nafteux P, Moons J, Coosemans W, Decker G, De Leyn P, Van Raemdonck D, Ectors N. Three-field lymphadenectomy for carcinoma of the esophagus and gastroesophageal junction in 174 R0 resections: impact on staging, disease-free survival, and outcome: a plea for adaptation of TNM classification in upper-half esophageal carcinoma. Ann Surg 2004; **240**: 962–974.

2. Ando N, Kato H, Igaki H, Shinoda M, Ozawa S, Shimizu H, Nakamura T, Yabusaki H, Aoyama N, Kurita A, Ikeda K, Kanda T, Tsujinaka T, Nakamura K, Fukuda H. A randomized trial comparing postoperative adjuvant chemotherapy with cisplatin and 5-fluorouracil versus preoperative chemotherapy for localized advanced squamous cell carcinoma of the thoracic esophagus (JCOG9907). Ann Surg Oncol 2012; **19**: 68-74.

3. Ando N, Iizuka T, Ide H, Ishida K, Shinoda M, Nishimaki T, Takiyama W, Watanabe H, Isono K, Aoyama N, Makuuchi H, Tanaka O, Yamana H, Ikeuchi S, Kabuto T, Nagai K, Shimada Y, Kinjo Y, Fukuda H. Surgery plus chemotherapy compared with surgery alone for localized squamous cell carcinoma of the thoracic esophagus: a Japan Clinical Oncology Group Study--JCOG9204. J Clin Oncol 2003; **21**: 4592-4596.

4. Tombran-Tink J, Chader CG, Johnson LV. PEDF: a pigment epithelium-derived factor with potent neuronal differentiative activity. Exp Eye Res 1991; **53**: 411-414.

5. Becerra SP, Sagasti A, Spinella P, Notario V. Pigment epithelium-derived factor behaves like a noninhibitory serpin. Neurotrophic activity does not require the serpin reactive loop. J Biol Chem 1995; **270**: 25992-25999.

6. Dawson DW, Volpert OV, Gillis P, Crawford SE, Xu H, Benedict W, Bouck NP. Pigment epithelium-derived factor: a potent inhibitor of angiogenesis. Science 1999; **285**: 245-248.

7. Raisler BJ, Berns KI, Grant MB, Beliaev D, Hauswirth WW. Adeno-associated virus type-2 expression of pigmented epithelium-derived factor or Kringles 1-3 of angiostatin reduce retinal neovascularization. Proc Natl Acad Sci U S A 2002; **99**: 8909-8914.

8. Doll JA, Stellmach VM, Bouck NP, Bergh AR, Lee C, Abramson LP, Cornwell ML, Pins MR, Borensztajn J, Crawford SE. Pigment epithelium-derived factor regulates the vasculature and mass of the prostate and pancreas. Nat Med 2003; **9**: 774-780.

9. Mahtabifard A, Merritt RE, Yamada RE, Crystal RG, Korst RJ. In vivo gene transfer of pigment epithelium-derived factor inhibits tumor growth in syngeneic murine models of thoracic malignancies. J Thorac Cardiovasc Surg 2003; **126**: 28-38.

10. Garcia M, Fernandez-Garcia NI, Rivas V, Carretero M, Escamez MJ, Gonzalez-Martin A, Medrano EE, Volpert O, Jorcano JL, Jimenez B, Larcher F, Del Rio M. Inhibition of xenografted human melanoma growth and prevention of metastasis development by dual antiangiogenic/antitumor activities of pigment epithelium-derived factor. Cancer Res 2004; **64**: 5632-5642.

11. Abe R, Shimizu T, Yamagishi S, Shibaki A, Amano S, Inagaki Y, Watanabe H, Sugawara H, Nakamura H, Takeuchi M, Imaizumi T, Shimizu. Overexpression of Pigment Epithelium-Derived Factor Decreases Angiogenesis and Inhibits the Growth of Human Malignant Melanoma Cells in Vivo. Am J Pathol 2004; **164**: 1225-1232.

12. Matsumoto K, Ishikawa H, Nishimura D, Hamasaki K, Nakao K, Eguchi K. Antiangiogenic property of pigment epithelium-derived factor in hepatocellular carcinoma. Hepatology 2004; **40**:252-259.

13. Zhang Y, Han J, Yang X, Shao C, Xu Z, Cheng R, Cai W, Ma J, Yang Z, Gao G. Pigment epithelium-derived factor inhibits angiogenesis and growth of gastric carcinoma by down-regulation of VEGF. Oncol Rep 2011; **26**: 681-686.

14. He SS, Shi HS, Yin T, Li YX, Luo ST, Wu QJ, Lu L, Wei YQ, Yang L. AAV-mediated gene transfer of human pigment epithelium-derived factor inhibits Lewis lung carcinoma growth in mice. Oncol Rep 2012; **27**: 1142-1148.
15. Wu QJ, Gong CY, Luo ST, Zhang DM, Zhang S, Shi HS, Lu L, Yan HX, He SS, Li DD, Yang L, Zhao X, Wei YQ. AAV-mediated human PEDF inhibits tumor growth and metastasis in murine colorectal peritoneal carcinomatosis model. BMC Cancer 2012; **12**:129. doi: 10.1186/1471-2407-12-129.
16. Shi HS, Yang LP, Wei W, Su XQ, Li XP, Li M, Luo ST, Zhang HL, Lu L, Mao YQ, Kan B, Yang L. Systemically administered liposome-encapsulated Ad-PEDF potentiates the anti-cancer effects in mouse lung metastasis melanoma. J Transl Med 2013; **11**: 86. doi: 10.1186/1479-5876-11-86.
17. Konson A, Pradeep S, Seger R. Phosphomimetic mutants of pigment epithelium-derived factor with enhanced antiangiogenic activity as potent anticancer agents. Cancer Res 2010; **70**: 6247–6257.
18. Uehara H, Miyamoto M, Kato K, Ebihara Y, Kaneko H, Hashimoto H, Murakami Y, Hase R, Takahashi R, Mega S, Shichinohe T, Kawarada Y, Itoh T, Okushiba S, Kondo S, Katoh H. Expression of Pigment epithelium-derived factor decreases liver metastasis and correlates with favorable prognosis for patients with ductal pancreatic adenocarcinoma. Cancer Res 2004; **64**: 3533-3537.
19. Hase R, Miyamoto M, Uehara H, Kadoya M, Ebihara Y, Murakami Y, Takahashi R, Mega S, Li L, Shichinohe T, Kawarada Y, Kondo S. Pigment epithelium-derived factor gene therapy inhibits human pancreatic cancer in mice. Clin Cancer Res 2005; **11**: 8737-8744.
20. Folkman J. Role of angiogenesis in tumor growth and metastasis. Semin Oncol 2002; **29**: 15-18.
21. Hanahan D, Folkman J. Patterns and emerging mechanisms of the angiogenic switch during tumorigenesis. Cell 1996; **86**:353-364.
22. Carmeliet P. Angiogenesis in life, disease and medicine. Nature 2005; **438**: 932-936.
23. Flamme I, Frölich T, Risau W. Molecular mechanisms of vasculogenesis and embryonic angiogenesis. J Cell Physiol 1997; **173**: 206–210.
24. Risau W. Mechanisms of angiogenesis. Nature 1997; **386**: 671–674.
25. Moore XL, Lu J, Sun L, Zhu CJ, Tan P, Wong MC. Endothelial progenitor cells' 'homing' specificity to brain tumors. Gene Ther 2004; **11**: 811-818.
26. Aghi M, Chiocca EA. Contribution of bone marrow-derived cells to blood vessels in ischemic tissues and tumors. Mol Ther 2005; **12**: 994-1005.
27. Spring H, Schüler T, Arnold B, Hämmerling GJ, Ganss R. Chemokines direct endothelial progenitors into tumor neovessels. Proc Natl Acad Sci U S A 2005; **102**: 18111-18116.
28. Duda DG, Cohen KS, Kozin SV, Perentes JY, Fukumura D, Scadden DT, Jain RK. Evidence for incorporation of bone marrow-derived endothelial cells into perfused blood vessels in tumors. Blood 2006; **107**:2774-2776.
29. Nolan DJ, Ciarrocchi A, Mellick AS, Jaggi JS, Bambino K, Gupta S, Heikamp E, McDevitt MR, Scheinberg DA, Benezra R, Mittal V. Bone marrow-derived endothelial progenitor cells are a major determinant of nascent tumor neovascularization. Genes Dev 2007; **21**: 1546-1558.
30. Abu El-Asrar AM, Struyf S, Verbeke H, Van Damme J, Geboes K. Circulating bone-marrow-derived endothelial precursor cells contribute to neovascularization in diabetic epiretinal membranes. Acta Ophthalmol 2011; **89**: 222–228.
31. Espinosa-Heidmann DG, Caicedo A, Hernandez EP, Csaky KG, Cousins SW. Bone marrow-derived progenitor cells contribute to experimental choroidal neovascularization. Invest Ophthalmol Vis Sci 2003; **44**: 4914–4919.

32. Longeras R, Farjo K, Ihnat M, Ma JX. A PEDF-derived peptide inhibits retinal neovascularization and blocks mobilization of bone marrow-derived endothelial progenitor cells. Exp Diabetes Res 2012; 518426. Published online 2011 June 28. doi: 10.1155/2012/518426.

33. Bagley RG, Walter-Yohrling J, Cao X, Weber W, Simons B, Cook BP, Chartrand SD, Wang C, Madden SL, Teicher BA. Endothelial precursor cells as a model of tumor endothelium: characterization and comparison with mature endothelial cells. Cancer Res 2003; **63**: 5866-5873.

34. Purhonen S, Palm J, Rossi D, Kaskenpää N, Rajantie I, Ylä-Herttuala S, Alitalo K, Weissman IL, Salven P. Bone marrow-derived circulating endothelial precursors do not contribute to vascular endothelium and are not needed for tumor growth. Proc Natl Acad Sci U S A 2008; **105**: 6620-6625.

35. Peters BA, Diaz LA, Polyak K, Meszler L, Romans K, Guinan EC, Antin JH, Myerson D, Hamilton SR, Vogelstein B, Kinzler KW, Lengauer C. Contribution of bone marrow-derived endothelial cells to human tumor vasculature. Nat Med 2005; **11**: 261-262.

36. Göthert JR, Gustin SE, van Eekelen JA, Schmidt U, Hall MA, Jane SM, Green AR, Göttgens B, Izon DJ, Begley CG. Genetically tagging endothelial cells in vivo: bone marrow-derived cells do not contribute to tumor endothelium. Blood 2004; **104**: 1769-1777.

37. Becerra SP, Notario V. The effects of PEDF on cancer biology: mechanisms of action and therapeutic potential. Nat Rev Cancer 2013; **13**:258-271.

38. Conway EM, Collen D and Carmeliet P. Molecular mechanisms of blood vessel growth. Cardiovasc Res 2001; **49**: 507-521.

39. Yancopoulos GD, Davis S, Gale NW, Rudge JS, Wiegand SJ and Holash J: Vascular-specific growth factors and blood vessel formation. Nature 2000; **407**: 242-248.

40. Yang LP, Cheng P, Peng XC, Shi HS, He WH, Cui FY, Luo ST, Wei YQ, Yang L. Anti-tumour effect of adenovirus-mediated gene transfer of pigment epithelium-derived factor on mouse B16-F10 melanoma. J Exp Clin Cancer Res 2009; **28**: 75, doi: 10.1186/1756-9966-28-75.

41. Takenaka K, Yamagishi S, Jinnouchi Y, Nakamura K, Matsui T, Imaizumi T. Pigment epithelium-derived factor (PEDF)-induced apoptosis and inhibition of vascular endothelial growth factor (VEGF) expression in MG63 human osteosarcoma cells. Life Sci 2005; **77**: 3231-3241.

42. Filleur S, Volz K, Nelius T, Mirochnik Y, Huang H, Zaichuk TA, Aymerich MS, Becerra SP, Yap R, Veliceasa D, Shroff EH, Volpert OV. Two functional epitopes of pigment epithelial-derived factor block angiogenesis and induce differentiation in prostate cancer. Cancer Res 2005; **65**: 5144-5152.

Fig.1

FACS analysis of PBMCs and EPCs.

A: Gating for PBMCs.

B: Exclusion gate for CD45+ cells.

C: Gating for negative control used isotype-matched rat immunoglobulin.

D: Representative analysis showing percentage of EPCs.

Fig.2

Western blot analysis of supernatant from human esophageal non-cancer cell line Het1A and human ESCC cell lines TE8 and HEC46, stably transfected with LV-PEDF or LV-GFP. As a positive control, 8ng of recombinant human PEDF protein (rhPEDF) was used. WT; wild type, G; transfected with LV-GFP, P; transfected with LV-PEDF, PC; positive control, S; supernatant, L; lysate.

Fig.3

In vitro HUVECs and HMVECs proliferation and migration assay. Columns, median of six independent experiments; bars, range. A value of 1.0 was determined as median of control value. C; control (medium alone), WT; wild type, G; transfected with LV-GFP, P; transfected with LV-PEDF. ＊; $p<0.05$, ＊＊; $p<0.01$.

Fig.4

A, F: Change every week of tumor volume of TE8WT, G, P and HEC46WT, G, P cells. Columns, median of tumor volume from six mice in each group; bars, range. W; wild type, G; transfected with LV-GFP, P; transfected with LV-PEDF.＊; $p<0.05$.

B: The representative photographs showing the effect of PEDF on the growth of subcutaneous cell implant models.

C, G: The representative microphotographs of immunohistochemical staining proving GFP and PEDF expression in each tumor tissue.

D, H: The representative microphotographs of immunohistochemical staining for CD34 in each tumor tissue.

E, I: Tumor microvessel densities in each tumor section. Columns, median of tumor microvessel densities in sections from six mice; bars, range. ＊＊; $p<0.01$.

J: Comparison of the microvessel densities in tumor tissue from TE8WT and HEC46WT subcutaneous tumor models. ＊; $p<0.05$.

Fig.5

A, B: The number of PBMCs and EPCs in the peripheral blood from mice subcutaneously xenografted TE8WT, G, P and HEC46WT, G, P cells. Columns, median of six mice; bars, range. ＊; $p<0.05$, ＊＊; $p<0.01$.

C, D: The representative fluorescence microscopic photographs of immunofluorescence staining for EPCs marker, CD31 (green) and Prominin Ⅰ (red) in tumor tissues derived from subcutaneously xenografted TE8WT, G, P and HEC46WT, G, P cells. CD31 and Prominin Ⅰ double-positive cells (merged image, yellow) indicate EPCs which form the tumor vessels. FITC- or Phycoerythrin-conjugated normal rat IgG was used as isotype controls.

E: Fields rate containing EPCs to total 25 fields at ×200 magnification per tissue sample extracted from six mice of each

group. WT; wild type, G; transfected with LV-GFP, P; transfected with LV-PEDF. A value of 1.0 shows median of WT value. All values are presented as median ±range. ＊＊ ; $p<0.01$.

Fig.1

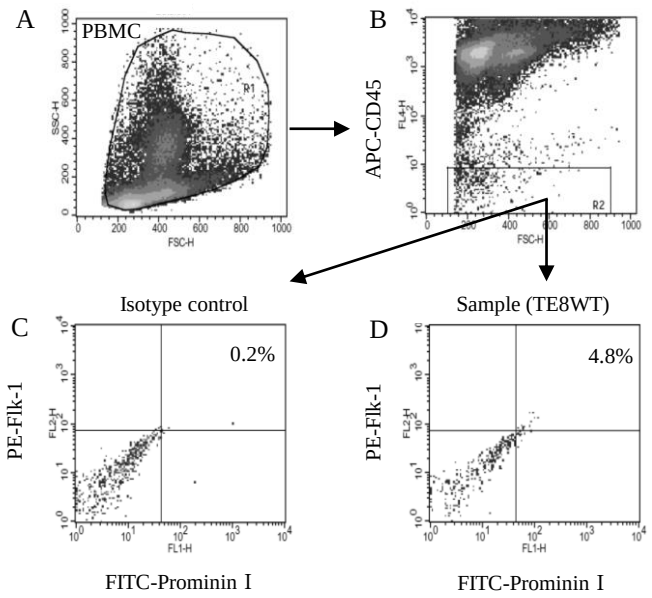
A
PBMC
R1
SSC-H
FSC-H
B
APC-CD45
R2
FSC-H
Isotype control
Sample (TE8WT)
C
0.2%
PE-Flk-1
FL2-H
FL1-H
FITC-Prominin I
D
4.8%
PE-Flk-1
FL2-H
FL1-H
FITC-Prominin I

Fig.2

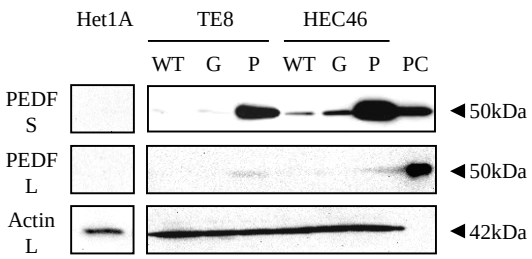
Het1A
TE8
HEC46
WT G P WT G P PC
PEDF S
50kDa
PEDF L
50kDa
Actin L
42kDa

Fig.3

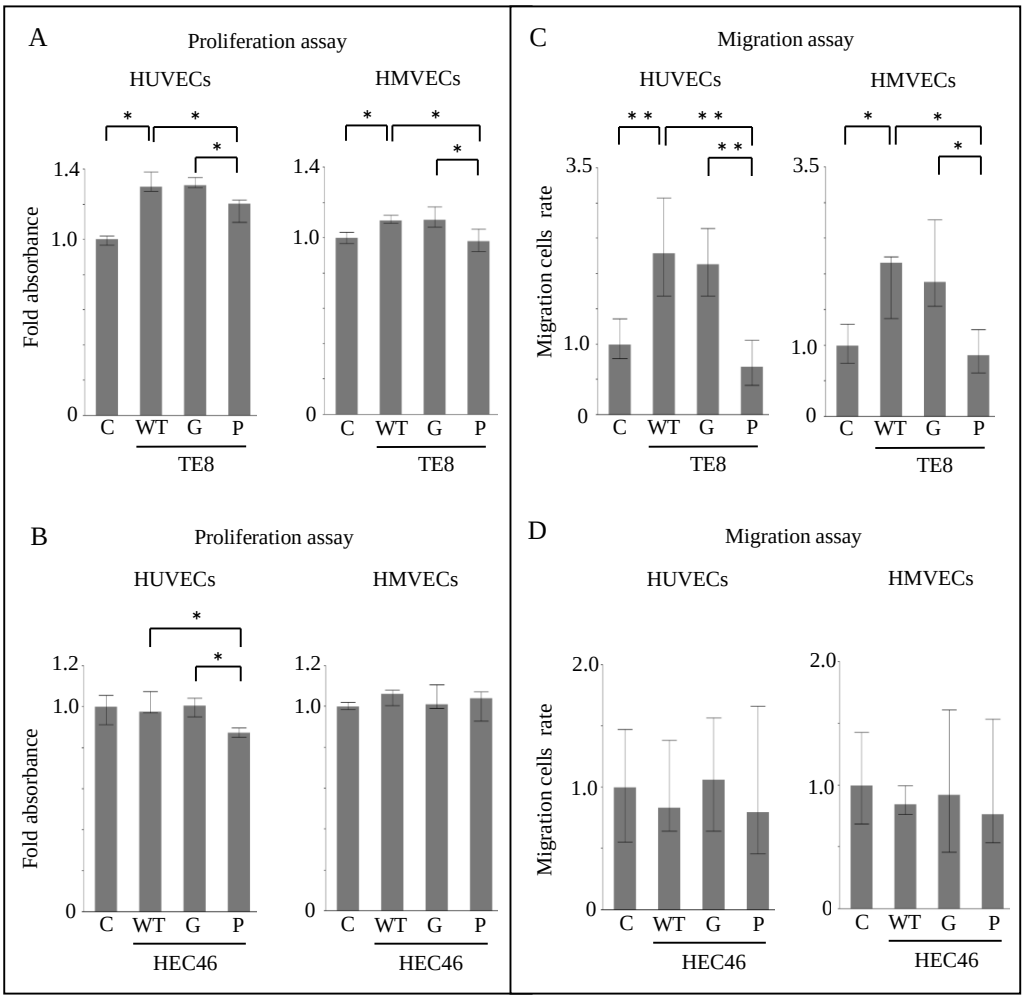
A
Proliferation assay
HUVECs
HMVECs
Fold absorbance
1.4
1.0
0
C WT G P
TE8
B
Proliferation assay
HUVECs
HMVECs
Fold absorbance
1.2
1.0
0
C WT G P
HEC46
C
Migration assay
HUVECs
HMVECs
Migration cells rate
3.5
1.0
0
C WT G P
TE8
D
Migration assay
HUVECs
HMVECs
Migration cells rate
2.0
1.0
0
C WT G P
HEC46

Fig.4

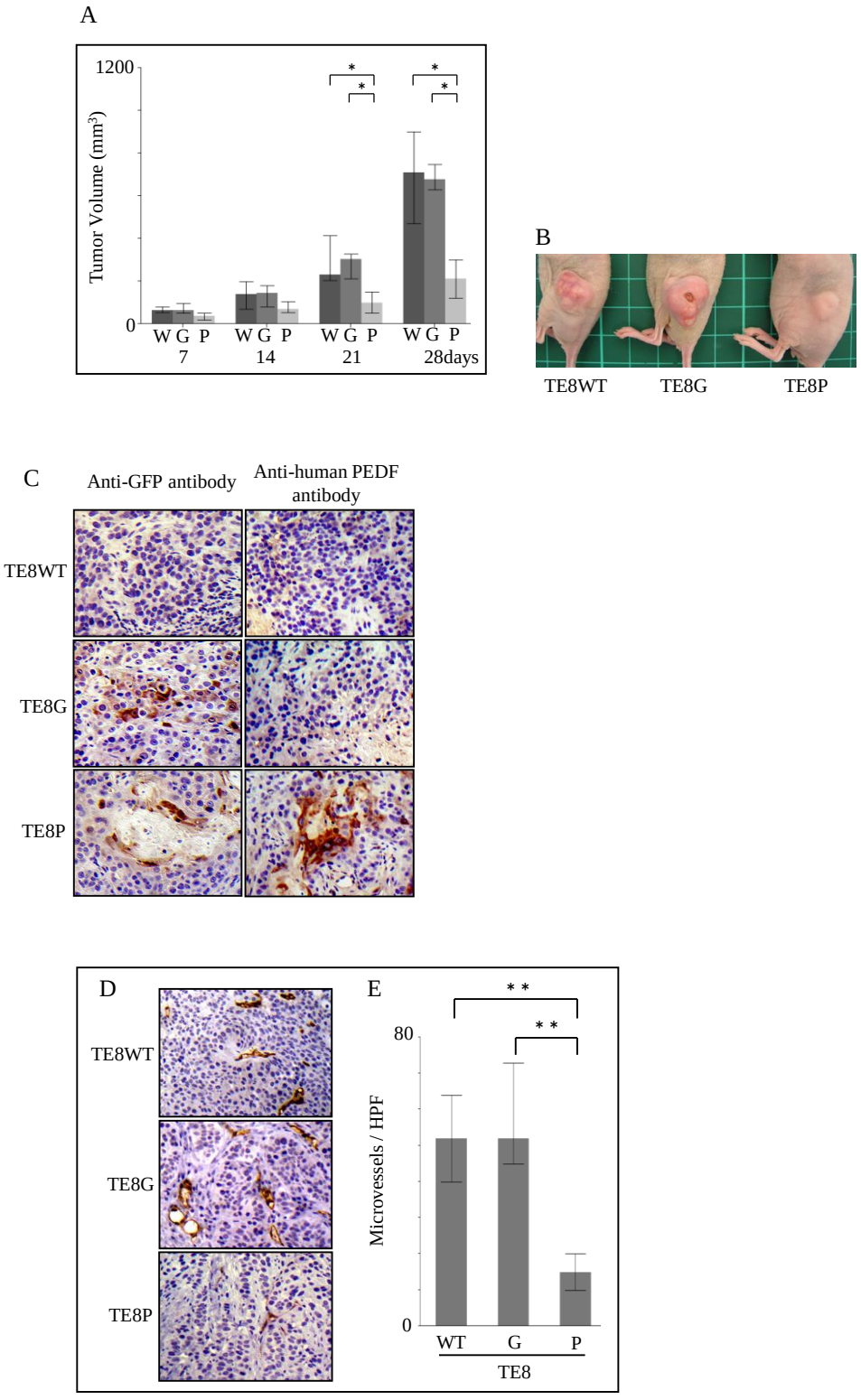
A
1200
0
Tumor Volume (mm3)
W G P
7
14
21
28days
*
B
TE8WT
TE8G
TE8P
C
Anti-GFP antibody
Anti-human PEDF antibody
TE8WT
TE8G
TE8P
D
E
80
0
Microvessels / HPF
WT
G
P
TE8

Fig.4

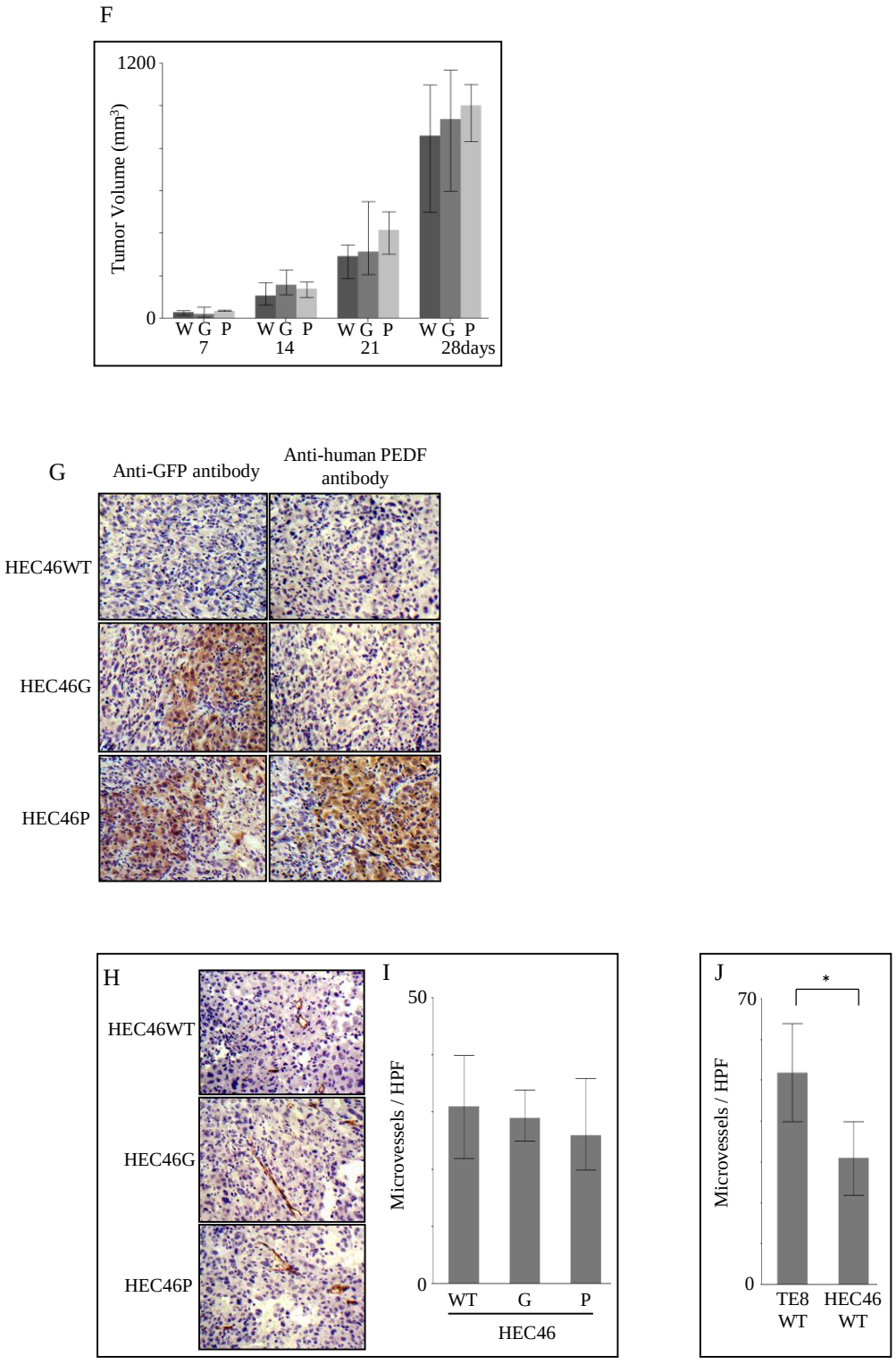
F
1200
0
Tumor Volume (mm3)
W G P
7
14
21
28days
G
Anti-GFP antibody
Anti-human PEDF antibody
HEC46WT
HEC46G
HEC46P
H
I
50
0
Microvessels / HPF
WT
G
P
HEC46
J
*
70
0
Microvessels / HPF
TE8 WT
HEC46 WT

Fig.5

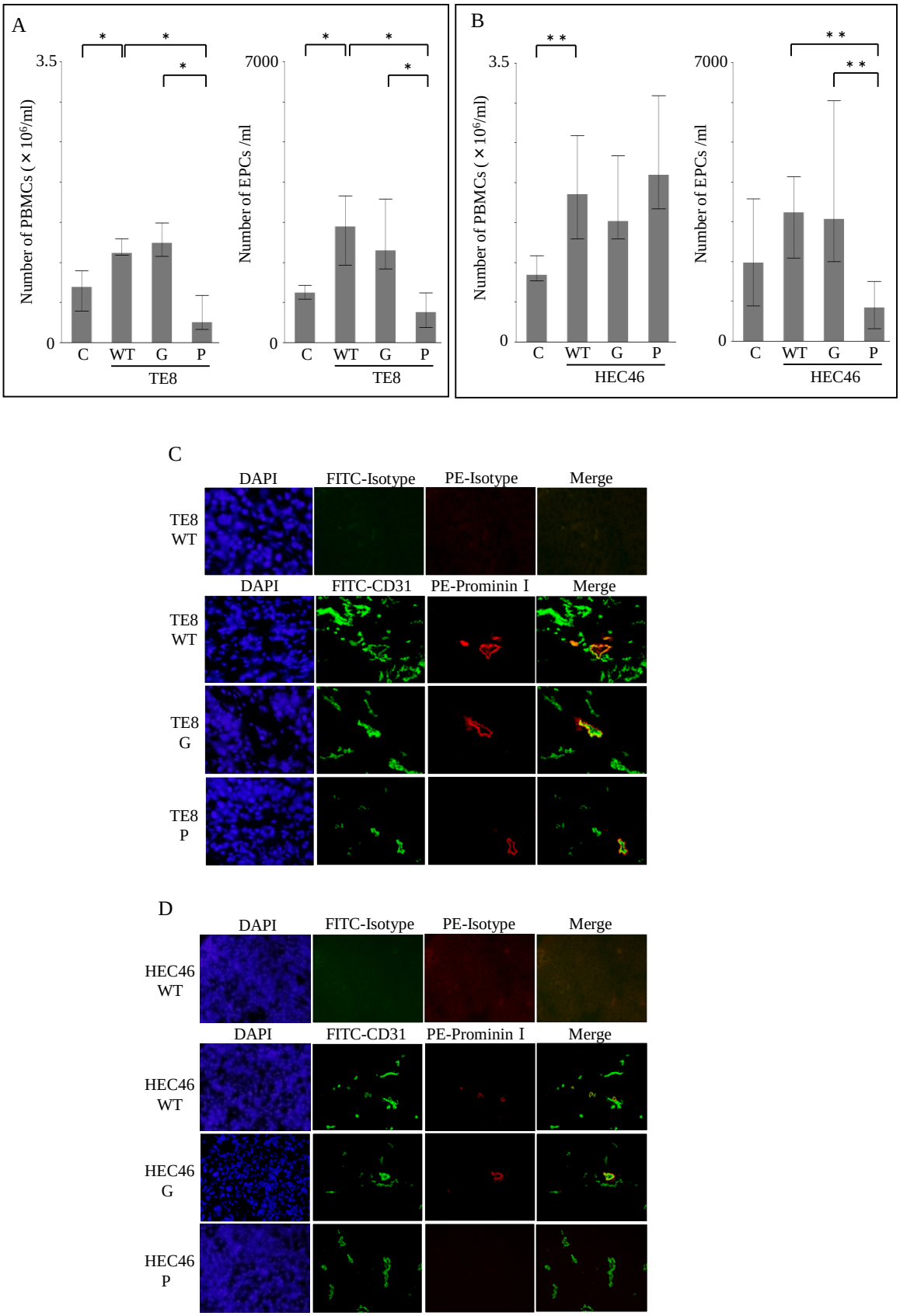
A
Number of PBMCs (× 10⁶/ml)
3.5
0
C
WT
G
P
TE8
Number of EPCs /ml
7000
0
C
WT
G
P
TE8
B
Number of PBMCs (× 10⁶/ml)
3.5
0
C
WT
G
P
HEC46
Number of EPCs /ml
7000
0
C
WT
G
P
HEC46
C
DAPI
FITC-Isotype
PE-Isotype
Merge
TE8 WT
DAPI
FITC-CD31
PE-Prominin I
Merge
TE8 WT
TE8 G
TE8 P
D
DAPI
FITC-Isotype
PE-Isotype
Merge
HEC46 WT
DAPI
FITC-CD31
PE-Prominin I
Merge
HEC46 WT
HEC46 G
HEC46 P

E

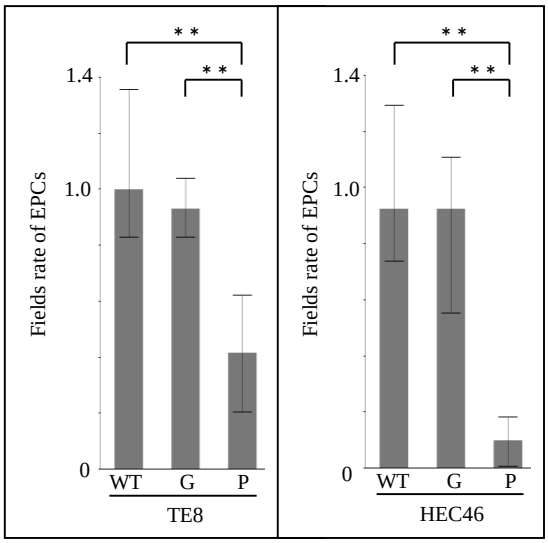
* *
* *
1.4
1.0
0
Fields rate of EPCs
WT
G
P
TE8
* *
* *
1.4
1.0
0
Fields rate of EPCs
WT
G
P
HEC46